Parametric Decay Instabilities during Electron Cyclotron Resonance Heating of Fusion Plasmas, Problems and Possibilities

S.K. Hansen[1,*], *S.K.* Nielsen[2], *J.* Stober[3], *J.* Rasmussen[2], *M.* Salewski[2], *M.* Willensdorfer[3], *M.* Hoelzl[3], *M.* Stejner[2], and the ASDEX Upgrade Team[4]

[1]Plasma Science and Fusion Center, Massachusetts Institute of Technology, Cambridge, MA 02139, USA
[2]Department of Physics, Technical University of Denmark, DK-2800 Kgs. Lyngby, Denmark
[3]Max-Planck-Institut für Plasmaphysik, D-85748 Garching b. München, Germany
[4]See Author List in H. Meyer for the ASDEX Upgrade Team, Nucl. Fusion **59**, 112014 (2019)

Abstract. We review parametric decay instabilities (PDIs) expected in connection with electron cyclotron resonance heating (ECRH) of magnetically confined fusion plasmas, with a specific focus on conditions relevant for the ITER tokamak. PDIs involving upper hybrid (UH) waves are likely to occur in O-mode ECRH scenarios at ITER if electron density profiles allowing trapping of UH waves near the ECRH frequency are present. Such PDIs may occur near the plasma center in ITER full-field scenarios heated by 170 GHz O-mode ECRH and on the high-field side of half-field ITER plasmas heated by 110 GHz or 104 GHz O-mode ECRH. Additionally, 110 GHz O-mode ECRH of half-field ITER scenarios may have low ECRH absorption, due to the electron cyclotron resonance being located on the high-field side of the main plasma. This potentially allows PDIs driven by a significant amount of ECRH radiation reaching the UH resonance in X-mode to occur, as X-mode radiation can be generated by reflection of unabsorbed O-mode radiation from the high-field side wall. The occurrence of PDIs during ECRH may damage microwave diagnostics, such as the electron cyclotron emission and low-field side reflectometer systems at ITER, as well as complicate the calculation of heating and current drive characteristics. However, if PDIs are induced in a controlled manner, they may provide novel diagnostic tools and allow the generation of a moderate fast ion population in plasmas heated only by ECRH.

1 Introduction

Parametric decay instabilities (PDIs) of millimeter wave radiation from gyrotron sources used for electron cyclotron resonance heating (ECRH) of magnetically confined fusion plasmas have been a topic of significant interest in recent years. The main reason for this is that PDIs can generate strong microwave signals capable of damaging microwave diagnostics [1], as well as transfering a significant fraction of the ECRH power from electromagnetic waves to quasi-electrostatic plasma waves, altering the heating and current drive characteristics from those expected based on linear ECRH theory [2, 3]. However, the microwave signals caused by PDIs can also serve as plasma diagnostics, e.g., allowing the occurrence of O-X-B heating to be confirmed [4, 5] and the properties of edge-localized modes to be explored [6]. Additionally, the low-frequency waves produced by some PDIs also allow generation of a moderate number of fast ions in pure ECRH plasmas [7–11]. In the present paper, we provide an overview of the ECRH PDIs studied in recent years and assess their potential impact on the O-mode ECRH scenarios planned for ITER [12].

In a PDI, a strong quasi-coherent pump wave, e.g., the millimeter waves used for ECRH in magnetic confinement fusion research, decays to two daughter waves once the pump wave amplitude exceeds a threshold determined by the nonlinear interaction strength between the three waves. Energy conservation in the three-wave process requires the frequency, f, and wave vector, $\mathbf{k}$, of the pump wave to equal the sum of those of the daughter waves, i.e.,

$$f_0 = f_1 + f_2, \quad \mathbf{k}_0 = \mathbf{k}_1 + \mathbf{k}_2, \tag{1}$$

where subscript 0 refers to the pump wave, while subscripts 1 and 2 refer to the daughter waves. Equation (1) requires the daughter waves excited by PDIs to be shifted in frequency relative to the pump wave, meaning that their frequencies will often be outside the protective diagnostic filters around the ECRH frequency in the case of ECRH PDIs. This is the root cause of the microwave diagnostics damage associated with such PDIs [1]. Traditionally, magnetic confinement fusion ECRH PDIs were only expected in connection with extremely high power ECRH provided by pulsed free-electron maser sources [13] or in scenarios with lower ECRH power where a significant fraction of the ECRH power would reach the upper hybrid resonance (UHR) with X-mode polarization [4, 5, 9–11, 14–30]. PDIs are expected in the above cases due to the occurrence of electric fields with large amplitudes. These large amplitude electric fields allow the convective losses normally suppressing PDIs in inhomogeneous plasmas [31–

*e-mail: soerenkh@psfc.mit.edu

33] to be overcome. In the free-electron maser case, the electric field amplitude is large enough to overcome the losses in the bulk plasma [13], while the UHR case relies on enhancement of the electric field amplitude associated with X-mode waves near the UHR, where their group velocity becomes very small [34]. Although PDIs involving X-mode waves reaching the UHR can occur at relatively low ECRH power levels without strict requirements on the plasma conditions [26, 27], they have generally only been considered to play a role in certain ECRH scenarios. This is due to the fact that X-mode waves cannot reach the UHR directly from the usual low-field side ECRH launcher position in tokamaks, owing to the R-cutoff always occurring on the low-field side of the UHR. The analysis of PDIs at the UHR is distinct for strongly overdense plasmas [18, 19, 22], commonly found in spherical tokamaks, and underdense/weakly overdense plasmas [17, 24–30], commonly found in conventional tokamaks and during plasma start-up, owing to the different dispersion properties of the electron Bernstein waves (EBWs) involved in the PDI in these cases. Specific scenarios in which PDIs at the UHR are of interest in connection with magnetic confinement fusion include fundamental X-mode [9–11, 17] and O-mode [9, 11, 21, 24–30] ECRH with optically thin/gray resonances, O-X-B heating [4, 5, 18–20], and EBW start-up [35–37].

In spite of previous expectations, strong PDI-like microwave signals were observed in connection with ECRH of plasma scenarios with tearing modes at the TEXTOR tokamak that did not fulfill any of the above criteria [38, 39]. This was explained in terms of ECRH PDIs involving trapped daughter waves [40], for which the convective losses normally limiting the occurrence of PDIs in inhomogeneous plasmas [31–33] are essentially removed. Specifically, the TEXTOR results at higher densities were explained in terms of decay of X-mode ECRH waves into two trapped UH waves near the O-point of the magnetic island [41–48], which has also been demonstrated at the ASDEX Upgrade tokamak [1, 6, 34], in low-temperature plasma filament experiments [2], and in particle-in-cell simulations [30, 49, 50]. The PDIs leading to microwave diagnostics damage at ASDEX Upgrade [1] and significant anomalous ECRH absorption in low-temperature plasma filaments [2] were both of the above type. More recently, an explanation of strong microwave signals observed at the Wendelstein 7-X stellarator in terms of decay of an X-mode ECRH wave into a trapped UH wave and a propagating X-mode wave around the O-point of a divertor island [51, 52], has also provided a potential explanation of the strong microwave signals observed at lower densities in TEXTOR [38, 39]. Apart from the PDIs driven by X-mode ECRH, PDIs driven by O-mode ECRH, relevant for the full-field ITER scenarios [12], have also been investigated. Particularly, decay of an O-mode ECRH wave to a trapped UH wave and a low-frequency lower hybrid wave has been investigated theoretically [53–56], in a low-temperature plasma filament [3], and at the FTU tokamak [57–59]. Additionally, it has recently been suggested that trapped low-frequency waves existing as a consequence of the strong gradients in the ITER and ASDEX Upgrade pedestals could lead to PDIs near the plasma edge during O-mode ECRH [60]. In this paper, we review the basic conditions under which the above PDIs may occur and assess their relevance for the O-mode ECRH scenarios proposed for ITER [12], in a manner similar to the investigations in Section 4 of [1], but covering different scenarios.

The remainder of the paper is organized as follows. Section 2 discusses the theoretical background of the employed criteria. In Section 3, the criteria are applied to the O-mode ECRH scenarios planned at ITER. Finally, Section 4 presents our conclusions.

2 Theoretical Background

ITER is a large tokamak with a minor radius $a = 2\,\mathrm{m}$ and a major radius $R_0 = 6.2\,\mathrm{m}$ [12]. The magnetic field strength, B, is approximately proportional to $1/R$, with R being the distance from the symmetry axis. Thus,

$$B \approx B_0 \frac{R_0}{R}, \tag{2}$$

where B_0 is the field at the magnetic axis; in full-field scenarios, $B_0 = 5.3\,\mathrm{T}$, while $B_0 = 2.65\,\mathrm{T}$ in half-field scenarios [12]. For quasi-perpendicular ECRH injection in the non-relativistic limit, absorption occurs when f_0 is equal to multiples of the electron cyclotron frequency [61],

$$|f_{ce}| = \frac{eB}{2\pi m_e} \approx \frac{eB_0}{2\pi m_e}\frac{R_0}{R}, \tag{3}$$

where e is the elementary charge and m_e is the electron mass. Additionally in the cold plasma limit, O-mode radiation has a cutoff at the electron plasma frequency,

$$f_{pe} = \sqrt{\frac{e^2 n_e}{4\pi^2 \epsilon_0 m_e}}, \tag{4}$$

where n_e is the electron density and ϵ_0 is the permittivity of vacuum. The UHR occurs for X-mode radiation at the UH frequency,

$$f_{UH} = \sqrt{f_{pe}^2 + f_{ce}^2}, \tag{5}$$

in cold plasmas, although we note that its properties are substantially influenced by warm plasma effects at electron temperatures $T_e \gtrsim 3\,\mathrm{keV}$ [1]. ECRH radiation with a frequency of f_0 will encounter the cold UHR ($f_0 = f_{UH}$) at an n_e value of

$$n_e^{UH} \approx \frac{\epsilon_0 m_e}{e^2}\left(4\pi^2 f_0^2 - \frac{e^2 B_0^2}{m_e^2}\frac{R_0^2}{R^2}\right). \tag{6}$$

We investigate n_e^{UH} for O-mode ECRH radiation at ITER, as such radiation may drive a PDI involving a trapped UH wave and a low-frequency lower hybrid wave in the presence of an inhomogeneous n_e profile with a local maximum slightly above n_e^{UH} [53–56]. Additionally, in connection with O-mode ECRH at ITER, we investigate whether scenarios are likely to occur in which a significant amount of X-mode radiation reaches the UHR upon reflection off the high-field side wall, as PDIs have been observed

in such scenarios at ASDEX Upgrade, even without UH wave trapping [23–27]. We note that the trapping-n_e of the UH wave is slightly different from the value in Eq. (6), since it is down-shifted relative to f_0 by the frequency of the low-frequency lower hybrid wave in accordance with Eq. (1). However, this shift can be ignored, as Eq. (6) already ignores finite-T_e effects, which will modify the UHR condition in the core of ITER plasmas [1, 12]. Equation (6) should thus be considered a rough estimate of the n_e-value at which UH wave trapping and field enhancement of X-mode ECRH waves may occur.

In addition to n_e^{UH}, we consider the n_e-limits and typical n_e-values at ITER. To avoid disruptions, n_e should not exceed the Greenwald density,

$$n_e^G\,[10^{20}\,\mathrm{m}^{-3}] = \frac{I_p\,[\mathrm{MA}]}{\pi(a\,[\mathrm{m}])^2}, \tag{7}$$

at the plasma edge [62–64]; I_p is the plasma current, which is 15 MA in standard full-field ITER scenarios and 7.5 MA in half-field ITER scenarios [12]. We note that the core-n_e can exceed n_e^G in the case of peaked plasma profiles obtained by pellet fueling [64] and that the empirical n_e^G given by Eq. (7) may underestimate the n_e-limit in ITER [65], meaning that n_e^G does not represent a hard limit on n_e in ITER, but still serves as a useful upper estimate of the edge-n_e. Further, the line-averaged n_e values leading to the minimum L−H threshold, $\bar{n}_e^{\min}$, which are representative of the lower bound of n_e in the core of typical H-mode plasmas, are given by $5\times10^{19}\,\mathrm{m}^{-3}$ in full-field ITER scenarios and $2.5\times10^{19}\,\mathrm{m}^{-3}$ in half-field ITER scenarios according to [12, 66].

3 Potential O-Mode ECRH PDI Scenarios at ITER

We plot n_e^{UH}, n_e^G, $\bar{n}_e^{\min}$, along with the (cold) fundamental ($f_0 = |f_{ce}|$) and second-harmonic ($f_0 = 2|f_{ce}|$) electron cyclotron resonances (ECRs) for the O-mode ECRH scenarios planned at ITER [12] in Fig. 1. The plots cover $R \in [4.11\,\mathrm{m}, 8.48\,\mathrm{m}]$, corresponding to the R-range of the ITER vacuum vessel in the midplane, while the R-ticks at $R_0 - a = 4.2\,\mathrm{m}$, $R_0 = 6.2\,\mathrm{m}$, and $R_0 + a = 8.2\,\mathrm{m}$ represent the extent of the main plasma in the midplane [12].

The top panel of Fig. 1 shows the situation for fundamental O-mode ECRH of the full-field ITER scenario ($B_0 = 5.3\,\mathrm{T}$, $I_p = 15\,\mathrm{MA}$) using the main ITER ECRH system operating at $f_0 = 170\,\mathrm{GHz}$ [12]. In this case, n_e^{UH} attains values from 0 to n_e^G in the central part of the plasma. Since the ECRH waves are injected from the low-field side (large R) [12] and thus encounter the region with $n_e^{UH} \in]0, n_e^G[$ before they are absorbed around the fundamental ECR, PDIs involving decay of the O-mode ECRH waves to trapped UH waves and low-frequency lower hybrid waves are likely occur if a region allowing UH wave trapping is present near the plasma center in full-field ITER scenarios. It is also possible to operate plasmas with core n_e-values approaching $2n_e^G$ when the plasma is fueled by pellets [64], in which case trapped UH wave PDIs may be possible over a wider range of the full-field ITER plasmas; the requirement that $n_e < n_e^G$ at the plasma edge means that there will always be some point with $R < R_0 + a$ at which $f_0 = f_{UH}$ in stable plasmas. Trapped UH wave PDIs in the ITER full-field scenarios may create strong microwave signals with frequency shifts $\sim 10\,\mathrm{GHz}$ from $f_0 = 170\,\mathrm{GHz}$ [1]. This makes them a potential risk to the ITER electron cyclotron emission (ECE) and low-field side reflectometer systems, operating in the frequency ranges 70−1000 GHz [67, 68] and 30−165 GHz [69], respectively. PDIs involving a significant amount of X-mode ECRH power reflected from the high-field side wall reaching the UHR are unlikely to occur in the full-field ITER scenario, as the fundamental ECR is located close to the plasma center and therefore expected to be optically thick for the O-mode ECRH waves [61].

The middle and bottom panels of Fig. 1 show the situation for fundamental O-mode ECRH of the half-field

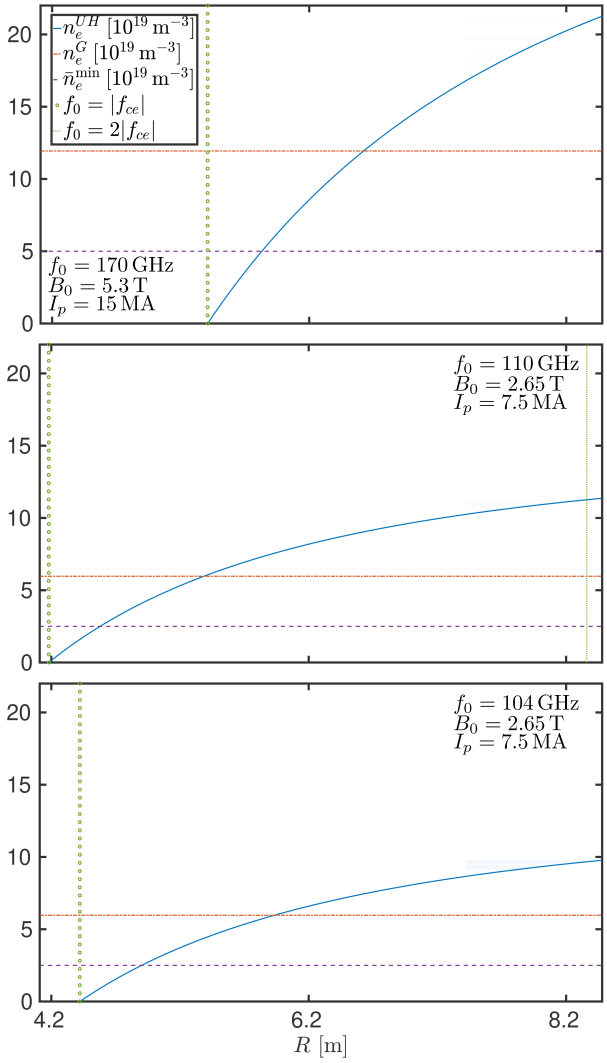

Figure 1. n_e^{UH}, n_e^G, $\bar{n}_e^{\min}$, $f_0 = |f_{ce}|$, and $f_0 = 2|f_{ce}|$ of the O-mode ECRH scenarios planned for ITER [12]. The top panel shows the situation for the full-field scenario ($B_0 = 5.3\,\mathrm{T}$, $I_p = 15\,\mathrm{MA}$) heated by the main ECRH system, $f_0 = 170\,\mathrm{GHz}$. The middle and bottom panels show the situations for O-mode ECRH of the half-field scenario ($B_0 = 2.65\,\mathrm{T}$, $I_p = 7.5\,\mathrm{MA}$) with $f_0 = 110\,\mathrm{GHz}$ and $f_0 = 104\,\mathrm{GHz}$, respectively.

ITER scenario ($B_0 = 2.65\,\mathrm{T}$, $I_p = 7.5\,\mathrm{MA}$) using the two lower-frequency ECRH options considered for ITER to enable ECRH start-up in the one-third-field scenarios [12], $f_0 = 110\,\mathrm{GHz}$ (middle panel) and $f_0 = 104\,\mathrm{GHz}$ (bottom panel). In these cases, n_e^{UH} covers the range from 0 to n_e^G on the high-field side of the plasma. Since the ECRH waves are still injected from the low-field side, they will encounter the region with $n_e^{UH} \in]0, n_e^G[$ before potentially being absorbed at the fundamental ECR [61]; the second-harmonic ECR occurring far on the low-field side, outside the main plasma, for $f_0 = 110\,\mathrm{GHz}$ is optically thin due to the low n_e and T_e in this region [61]. This means that 110 GHz and 104 GHz ECRH waves are also likely to drive PDIs involving decay of the O-mode ECRH waves into trapped UH waves and low-frequency lower hybrid waves in regions allowing UH wave trapping on the high-field side in ITER half-field scenarios. Such trapped UH wave PDIs would again pose a risk to the ECE [67, 68] and low-field side reflectometer [69] systems at ITER. Operation with pellet fueling above n_e^G would allow the trapped UH wave PDIs to occur near the plasma center and on the low-field side in addition to the high-field side; once again, the requirement of $n_e < n_e^G$ at the plasma edge means that there will always be some point with $R < R_0 + a$ at which $f_0 = f_{UH}$ in stable plasmas. While the $f_0 = 110\,\mathrm{GHz}$ and $f_0 = 104\,\mathrm{GHz}$ cases are similar in terms of their behavior with respect to PDIs involving a trapped UH wave, the conclusions regarding the possibility of having a significant amount of X-mode radiation reaching the UHR due to reflections from the high-field side wall and driving PDIs differ. For $f_0 = 110\,\mathrm{GHz}$, the middle panel of Fig. 1 shows that the fundamental ECR is located on the far high-field side, slightly outside the main plasma, meaning that its absorption is highly dependent on the precise value of B_0 and the angle at which the O-mode ECRH waves are launched [24–27, 61]. If virtually no particles inside the last closed flux surface are able to fulfill the ECR resonance condition [61], a significant amount of the injected O-mode radiation may reflect off the high-field side wall and (for a specific range of angles, which can be computed using [24]) re-enter the plasma as X-mode radiation that can drive PDIs at the UHR [17, 24–27]. This mechanism has been demonstrated experimentally in ASDEX Upgrade [24–27] and can be assessed for given ITER plasma conditions and ECRH beam geometries using the theory of [24]. We note that by slightly increasing B_0 such that the fundamental ECR occurs inside the last closed flux surface at the midplane, the absorption of 110 GHz ECRH radiation from the midplane launchers can be made more certain, which should also limit the occurrence of PDIs relying on X-mode radiation reaching the UHR. The minimum value of B_0 at which ECR absorption around the midplane is guaranteed, $B_0^{\min}$, is given by the condition that $f_0 = |f_{ce}|$ at $R = R_0 - a$, from which Eq. (3) yields

$$B_0^{\min} \approx 2\pi f_0 \frac{m_e}{e} \frac{R_0 - a}{R_0}. \tag{8}$$

For $f_0 = 110\,\mathrm{GHz}$, we find $B_0^{\min} \approx 2.66\,\mathrm{T}$, so operating at B_0 slightly above 2.65 T should prevent the occurrence of PDIs relying on a significant amount of X-mode ECRH power reaching the UHR. In the case of $f_0 = 104\,\mathrm{GHz}$, shown in the bottom panel of Fig. 1, the fundamental ECR occurs well inside main plasma around the midplane for $B_0 = 2.65\,\mathrm{T}$, so no PDIs relying on X-mode ECRH waves reaching the UHR are expected in this case. Additionally, $B_0^{\min} \approx 2.52\,\mathrm{T}$ for $f_0 = 104\,\mathrm{GHz}$, meaning that operation at B_0 values somewhat below 2.65 T is also possible without the occurrence of PDIs relying on X-mode ECRH power around the UHR.

4 Conclusion

We have investigated the potential occurrence of PDIs in O-mode ECRH scenarios at ITER [12], using an approach similar to that employed for the ITER X-mode ECRH scenarios in Section 4 of [1]. We found that PDIs are likely to occur near the UHR in connection with phenomena leading to non-monotonic n_e-profiles allowing UH wave trapping in a wide variety of O-mode ECRH scenarios at ITER, as well as in situations with X-mode radiation reflected off the high-field side wall reaching the UHR without restrictions on the n_e-profiles in scenarios with limited ECRH absorption. Specifically, trapped UH wave PDIs may occur near the plasma center during 170 GHz ECRH in full-field scenarios ($B_0 = 5.3\,\mathrm{T}$, $I_p = 15\,\mathrm{MA}$), while PDIs requiring limited ECRH absorption are unlikely in these scenarios. Trapped UH wave PDIs may also occur on the high-field side during 110 GHz or 104 GHz ECRH of half-field scenarios ($B_0 = 2.65\,\mathrm{T}$, $I_p = 7.5\,\mathrm{MA}$). Such scenarios may further allow PDIs requiring limited ECRH absorption at sufficiently low B_0. For 110 GHz ECRH, a $B_0 > 2.66\,\mathrm{T}$ was found to make such PDIs unlikely for ECRH beams launched from the outboard midplane, while a less strict requirement of $B_0 > 2.52\,\mathrm{T}$ was found to apply for 104 GHz ECRH. It is possible to mitigate the potential damage to microwave diagnostics due to ECRH PDIs by installing additional filters around the frequencies expected to be affected and by minimizing the abilitiy of the radiometers to pick up strong signals generated in the ECRH beams [1].

While trapped UH wave PDIs have been found to lead to diagnostics damage [1] and significant anomalous ECRH absorption [2, 3], which would generally be detrimental to the operation of the ITER ECRH system, we note that PDIs may also allow novel diagnostics and heating schemes to be implemented. For instance, PDIs involving X-mode radiation reaching the UHR are being considered for generating fast ions with ECRH in spherical tokamaks [7, 8], although we note that the efficacy of this scheme has yet to be demonstrated, and trapped UH wave PDIs occurring near the plasma edge have already been used to investigate edge-localized mode and L-mode blob characteristics at ASDEX Upgrade [6]. Since PDIs involving low-frequency trapped waves in the density pedestal are expected in connection with O-mode ECRH at ITER [60], it would be of particular interest to assess their value as an edge diagnostic.

Acknowledgements

SKH acknowledges support by an Internationalisation Fellowship (CF19-0738) from the Carlsberg Foundation. This work was supported by a research grant (15483) from VILLUM FONDEN. This work has been carried out within the framework of the EUROfusion Consortium, funded by the European Union via the Euratom Research and Training Programme (Grant Agreement No 101052200 — EUROfusion). Views and opinions expressed are however those of the author(s) only and do not necessarily reflect those of the European Union or the European Commission. Neither the European Union nor the European Commission can be held responsible for them.

References

[1] S.K. Hansen, A.S. Jacobsen, M. Willensdorfer, S.K. Nielsen, J. Stober, K. Höfler, M. Maraschek, R. Fischer, M. Dunne, the EUROfusion MST1 team et al., Plasma Phys. Control. Fusion **63**, 095002 (2021)

[2] A.B. Altukhov, V.I. Arkhipenko, A.D. Gurchenko, E.Z. Gusakov, A.Yu. Popov, L.V. Simonchik, M.S. Usachonak, EPL **126**, 15002 (2019)

[3] L. Simonchik, A. Altukhov, V. Arkhipenko, A. Gurchenko, E. Gusakov, A. Popov, M. Usachonak, Europhys. Conf. Abstracts **43C**, P2.4012 (2019)

[4] H.P. Laqua, V. Erckmann, H.J. Hartfuß, H. Laqua, W7-AS Team, ECRH Group, Phys. Rev. Lett. **78**, 3467 (1997)

[5] H.P. Laqua, Plasma Phys. Control. Fusion **49**, R1 (2007)

[6] S.K. Hansen, S.K. Nielsen, J. Stober, J. Rasmussen, M. Stejner, M. Hoelzl, T. Jensen, the ASDEX Upgrade team, Nucl. Fusion **60**, 106008 (2020)

[7] M. Gryaznevich, A. Nicolai, V. Chuyanov, Tokamak Energy Ltd. Team, Probl. At. Sci. Technol. Ser. Thermonucl. Fusion **44**, 107 (2021)

[8] S.K. Nielsen, M.P. Gryaznevich, A.S. Jacobsen, T. Jensen, M. Jessen, S.B. Korsholm, J. Rasmussen, M. Salewski, M.G. Senstius, V. Naulin et al., Fusion Eng. Des. **166**, 112288 (2021)

[9] R. Wilhelm, V. Erckmann, G. Janzen, W. Kasparek, G. Müller, E. Räuchle, P.G. Schüller, K. Schwörer, M. Thumm, the W VII-A team, Plasma Phys. Control. Fusion **26**, 1433 (1984)

[10] D.G. Bulyginskii, V.V. D'yachenko, M.A. Irzak, M.M. Larionov, L.S. Levin, G.A. Serebrenyi, N.V. Shustova, Sov. J. Plasma Phys. **12**, 77 (1986)

[11] Z.A. Pietrzyk, A. Pochelon, R. Behn, A. Bondeson, M. Dutch, T.P. Goodman, M.Q. Tran, D.R. Whaley, Nucl. Fusion **33**, 197 (1993)

[12] ITER Organization, Tech. Rep. ITR-18-003, ITER Organization, St. Paul-lez-Durance (2018), `https://www.iter.org/technical-reports`

[13] M. Porkolab, B.I. Cohen, Nucl. Fusion **28**, 239 (1988)

[14] S. Hiroe, H. Ikegami, Phys. Rev. Lett. **19**, 1414 (1967)

[15] B. Grek, M. Porkolab, Phys. Rev. Lett. **30**, 836 (1973)

[16] M. Okabayashi, K. Chen, M. Porkolab, Phys. Rev. Lett. **31**, 1113 (1973)

[17] F.S. McDermott, G. Bekefi, K.E. Hackett, J.S. Levine, M. Porkolab, Phys. Fluids **25**, 1488 (1982)

[18] V. Shevchenko, G. Cunningham, A. Gurchenko, E. Gusakov, B. Lloyd, M. O'Brien, A. Saveliev, A. Surkov, F. Volpe, M. Walsh, Fusion Sci. Technol. **52**, 202 (2007)

[19] E.Z. Gusakov, A.V. Surkov, Plasma Phys. Control. Fusion **49**, 631 (2007)

[20] A. Köhn, G. Birkenmeier, A. Chusov, P. Diez, A. Feuer, U. Höfel, H. Höhnle, E. Holzhauer, W. Kasparek, S. Merli et al., Plasma Phys. Control. Fusion **55**, 014010 (2013)

[21] S. Kubo, M. Nishiura, K. Tanaka, D. Moseev, S. Ogasawara, T. Shimozuma, Y. Yoshimura, H. Igami, H. Takahashi, T.I. Tsujimura et al., J. Instrum. **11**, C06005 (2016)

[22] A.V. Arefiev, I.Y. Dodin, A. Köhn, E.J. Du Toit, E. Holzhauer, V.F. Shevchenko, R.G.L. Vann, Nucl. Fusion **57**, 116024 (2017)

[23] S.K. Nielsen, P.K. Michelsen, S.K. Hansen, S.B. Korsholm, F. Leipold, J. Rasmussen, M. Salewski, M. Schubert, M. Stejner, J. Stober et al., Phys. Scr. **92**, 024001 (2017)

[24] S.K. Hansen, S.K. Nielsen, M. Salewski, M. Stejner, J. Stober, the ASDEX Upgrade team, Plasma Phys. Control. Fusion **59**, 105006 (2017)

[25] S.K. Hansen, S.K. Nielsen, M. Salewski, M. Stejner, J. Stober, the ASDEX Upgrade team, EPJ Web Conf. **149**, 03020 (2017)

[26] S.K. Hansen, S.K. Nielsen, J. Stober, J. Rasmussen, M. Stejner, the ASDEX Upgrade team, EPJ Web Conf. **203**, 02007 (2019)

[27] S.K. Hansen, S.K. Nielsen, J. Stober, J. Rasmussen, M. Salewski, M. Stejner, ASDEX Upgrade Team, Phys. Plasmas **26**, 062102 (2019)

[28] M.G. Senstius, S.K. Nielsen, R.G.L. Vann, EPJ Web Conf. **203**, 01010 (2019)

[29] M.G. Senstius, S.K. Nielsen, R.G. Vann, S.K. Hansen, Plasma Phys. Control. Fusion **62**, 025010 (2020)

[30] M.G. Senstius, Ph.D. thesis, Technical University of Denmark, Kgs. Lyngby (2020), `https://orbit.dtu.dk/files/239590925/MGSenstius_PhD_Thesis.pdf`

[31] A.D. Piliya, *Decay Instability in Weakly Inhomogeneous Plasma*, in *Proc. 10th Int. Conf. Phenomena in Ionized Gases (Oxford)*, edited by R.N. Franklin (Donald Parsons & Co. Ltd., Oxford, 1971), p. 320

[32] M.N. Rosenbluth, Phys. Rev. Lett. **29**, 565 (1972)

[33] A.D. Piliya, Sov. Phys.–JETP **37**, 629 (1973)

[34] S.K. Hansen, Ph.D. thesis, Technical University of Denmark, Kgs. Lyngby (2019),

https://pure.mpg.de/rest/items/item_3182239/component/file_3182252/content

[35] V. Shevchenko, M.R. O'Brien, D. Taylor, A.N. Saveliev, MAST Team, Nucl. Fusion **50**, 022004 (2010)

[36] V.F. Shevchenko, Y.F. Baranov, T. Bigelow, J.B. Caughman, S. Diem, C. Dukes, P. Finburg, J. Hawes, C. Gurl, J. Griffiths et al., EPJ Web Conf. **87**, 02007 (2015)

[37] N.A. Lopez, F.M. Poli, Plasma Phys. Control. Fusion **60**, 065007 (2018)

[38] E. Westerhof, S.K. Nielsen, J.W. Oosterbeek, M. Salewski, M.R. De Baar, W.A. Bongers, A. Bürger, B.A. Hennen, S.B. Korsholm, F. Leipold et al., Phys. Rev. Lett. **103**, 125001 (2009)

[39] S.K. Nielsen, M. Salewski, E. Westerhof, W. Bongers, S.B. Korsholm, F. Leipold, J.W. Oosterbeek, D. Moseev, M. Stejner, the TEXTOR team, Plasma Phys. Control. Fusion **55**, 115003 (2013)

[40] E.Z. Gusakov, V.I. Fedorov, Sov. J. Plasma Phys. **5**, 463 (1979)

[41] A.Yu. Popov, E.Z. Gusakov, Plasma Phys. Control. Fusion **57**, 025022 (2015)

[42] E.Z. Gusakov, A.Yu. Popov, Phys. Plasmas **23**, 082503 (2016)

[43] E.Z. Gusakov, A.Yu. Popov, Nucl. Fusion **59**, 104003 (2019)

[44] E.Z. Gusakov, A.Yu. Popov, P.V. Tretinnikov, Nucl. Fusion **59**, 106040 (2019)

[45] E.Z. Gusakov, A.Yu. Popov, Plasma Phys. Control. Fusion **62**, 025028 (2020)

[46] E.Z. Gusakov, A.Yu. Popov, Phys. Plasmas **27**, 082502 (2020)

[47] E.Z. Gusakov, A.Yu. Popov, Plasma Phys. Control. Fusion **63**, 125017 (2021)

[48] E.Z. Gusakov, A.Yu. Popov, Plasma Phys. Rep. **48**, 327 (2022)

[49] M.G. Senstius, S.K. Nielsen, R.G.L. Vann, Phys. Plasmas **27**, 062102 (2020)

[50] M.G. Senstius, S.K. Nielsen, R.G.L. Vann, Plasma Phys. Control. Fusion **63**, 065018 (2021)

[51] A. Tancetti, Ph.D. thesis, Technical University of Denmark, Kgs. Lyngby (2021), https://backend.orbit.dtu.dk/ws/portalfiles/portal/274567494/PhD_Thesis.pdf

[52] A. Tancetti, S.K. Nielsen, J. Rasmussen, E.Z. Gusakov, A.Yu. Popov, D. Moseev, T. Stange, M.G. Senstius, C. Killer, M. Vecséi et al., Nucl. Fusion **62**, 074003 (2022)

[53] E.Z. Gusakov, A.Yu. Popov, A.N. Saveliev, E.V. Sysoeva, Plasma Phys. Control. Fusion **59**, 075002 (2017)

[54] E.Z. Gusakov, A.Yu. Popov, Phys. Plasmas **25**, 012101 (2018)

[55] E.Z. Gusakov, A.Yu. Popov, A.N. Saveliev, Plasma Phys. Control. Fusion **61**, 025006 (2019)

[56] E.Z. Gusakov, A.Yu. Popov, Plasma Phys. Control. Fusion **63**, 015016 (2021)

[57] A. Bruschi, E. Alessi, W. Bin, O. D'Arcangelo, B. Baiocchi, F. Belli, G. Calabrò, I. Casiraghi, V. Cocilovo, L. Figini et al., Nucl. Fusion **57**, 076004 (2017)

[58] A. Bruschi, E. Alessi, B. Baiocchi, W. Bin, O. D'Arcangelo, F. Fanale, L. Figini, C. Galperti, S. Garavaglia, G. Gittini et al., EPJ Web Conf. **203**, 02005 (2019)

[59] B. Baiocchi, W. Bin, A. Bruschi, L. Figini, U. Tartari, E. Alessi, O. D'Arcangelo, J. Instrum. **15**, C01046 (2020)

[60] E.Z. Gusakov, A.Yu. Popov, Phys. Rev. Lett. **128**, 065001 (2022)

[61] M. Bornatici, R. Cano, O. De Barbieri, F. Engelmann, Nucl. Fusion **23**, 1153 (1983)

[62] M. Greenwald, J.L. Terry, S.M. Wolfe, S. Ejima, M.G. Bell, S.M. Kaye, G.H. Neilson, Nucl. Fusion **28**, 2199 (1988)

[63] M. Greenwald, Plasma Phys. Control. Fusion **44**, R27 (2002)

[64] P.T. Lang, C. Angioni, M. Bernert, A. Bock, T.M.J. Engelhardt, R. Fischer, O.J.W.F. Kardaun, B. Ploeckl, M. Prechtl, W. Suttrop et al., Nucl. Fusion **60**, 092003 (2020)

[65] M. Giacomin, A. Pau, P. Ricci, O. Sauter, T. Eich, the ASDEX Upgrade team, JET Contributors, the TCV team, Phys. Rev. Lett. **128**, 185003 (2022)

[66] Y.R. Martin, T. Takizuka, ITPA CDBM H-mode Threshold Database Working Group, J. Phys.: Conf. Ser. **123**, 012033 (2008)

[67] V.S. Udintsev, S. Danani, G. Taylor, T. Giacomin, J. Guirao, S. Pak, S. Hughes, L. Worth, G. Vayakis, M.J. Walsh et al., EPJ Web Conf. **203**, 03003 (2019)

[68] Y. Liu, V.S. Udintsev, S. Danani, G. Paraiso, G. Taylor, M.E. Austin, A. Basile, J.H. Beno, B. Bunkowski, R. Feder et al., J. Instrum. **17**, C04019 (2022)

[69] C.M. Muscatello, C. Anderson, J. Anderson, A. Basile, R.L. Boivin, M. Duco, D.K. Finkenthal, A. Gattuso, J. Klabacha, G.J. Kramer et al., Nucl. Fusion **60**, 066005 (2020)